



THE UNIVERSITY *of* EDINBURGH

Edinburgh Research Explorer

Accounting for false mortality in telemetry tag applications

Citation for published version:

Bird, T, Lyon, J, Wotherspoon, S, King, R & McCarthy, M 2017, 'Accounting for false mortality in telemetry tag applications', *Ecological Modelling*, vol. 355, pp. 116-125.
<https://doi.org/10.1016/j.ecolmodel.2017.01.019>

Digital Object Identifier (DOI):

[10.1016/j.ecolmodel.2017.01.019](https://doi.org/10.1016/j.ecolmodel.2017.01.019)

Link:

[Link to publication record in Edinburgh Research Explorer](#)

Document Version:

Peer reviewed version

Published In:

Ecological Modelling

General rights

Copyright for the publications made accessible via the Edinburgh Research Explorer is retained by the author(s) and / or other copyright owners and it is a condition of accessing these publications that users recognise and abide by the legal requirements associated with these rights.

Take down policy

The University of Edinburgh has made every reasonable effort to ensure that Edinburgh Research Explorer content complies with UK legislation. If you believe that the public display of this file breaches copyright please contact openaccess@ed.ac.uk providing details, and we will remove access to the work immediately and investigate your claim.



Accounting for false mortality in telemetry tag applications

Tomas Bird ^{*1}, Jarod Lyon ², Simon Wotherspoon³, Ruth King⁴, and Michael McCarthy ¹

¹Department of Botany, University of Melbourne, Australia

²Arthur Rylah Institute, Department of Sustainability and Environment, Australia

³Institute of Marine and Antarctic Studies, University of Tasmania, Australia

⁴School of Mathematics, University of Edinburgh, United Kingdom

December 5, 2016

1. Abstract

Deaths of animals in the wild are rarely observed directly, which often limits understanding of survival rates. Telemetry transmitters offer field ecologists the opportunity to observe mortality events in cases as the absence of animal movement. When observations of mortality are based on factors such as the absence of animal movement, live individuals can be mistaken for dead, resulting in biased estimates of survival. Additionally, tag failure or emigration might also influence estimates of survival in telemetry studies. Failing to account for mis-classification, tag failure, and emigration rates can result in overestimates of mortality rates by up two-fold, even when the data are corrected for obviously mistaken entries. We use a multi-state capture-recapture model with a misclassification parameter in estimating both the rate of permanent emigration and/or tag failure and the rate at which individuals are mistakenly identified as dead. We use this method on an annual telemetry survey of three species of native fish in the Murray river, Australia: Murray cod (*Maccullochella peelii*), trout cod (*Maccullochella macquariensis*) and golden perch (*Macquaria ambigua*). Evidence for higher mortality rates in the first year post-implantation occurred for Murray cod and golden perch, which is likely an effect of tagging and/or the transmitter, or transmitters shedding. Using simulations, we confirm that our model approach is robust to a broad range of misclassification and transmitter failure rates. With these simulations we also demonstrate that misclassification models that do not account for emigration will likely be erroneous if live and dead animals have different probabilities of detection. These findings will have a broad interest to ecologists wishing to account for multiple sources of misclassification error in capture-mark-recapture studies, with the caveat that the specifics of the approach are dependent on species, transmitter types and other aspects of experimental design which may or may not be amenable to the misclassification framework.

2. Introduction

Many ecological studies focus on estimating survival rates of animals in wild populations. However, mortality events are rarely if ever observed using standard sampling approaches. Survival rates can be estimated in the wild from capture-mark-recapture

(CMR) experiments (25), based on several core assumptions surrounding how effective sampling is at capturing animals. First, CMR experimental design assumes that individuals in the population have equal probability of capture, or that this probability can readily be modelled as a function of known characteristics. Similarly, marks or transmitters are assumed to remain affixed to all individuals, and all individuals are assumed to remain in the study area. Based on these assumptions, the sizes of populations can be estimated by marking individuals on successive capture occasions (). By repeating the capture and implantation process over multiple equally-spaced intervals, the rate of permanent departures from the tagged population can be estimated, the basic principle being that within increasing numbers of failed recaptures, the likelihood that the observed lack of captures is due to repeated failures is eclipsed by the likelihood of their having left the population.

With populations that are easily captured, the two likelihoods of permanent departure versus repeated failed detection are relatively easy to distinguish over shorter timeframes. However in many wild populations, excessive sampling effort can be required to make the distinction (28). In such cases, alternative experimental designs can be used to reduce the effort required to accurately estimate mortality rates. Recently, telemetry and satellite tags that allow accurate observations of animal locations remotely have been used to estimate mortality in hard-to-capture populations (5). Extending the use-cases of telemetry tags, mortality events can also be inferred from cessation of individual tag movement (20). In addition, some kinds of tags are equipped with a 'mortality switch', which emit a unique signal when the implanted individual fails to move for an extended period or if the tag is dropped from the implanted individual (3).

In all cases where telemetry tags are used to infer mortality, animal motion is an important proximal observation, whereby lack of movement can be used to imply mortality. However, experimental design must take into account the obvious ambiguities possible in interpreting these data. For example, studies inferring mortality from swimming speed (6), depth (32) and diel movement (9) have all noted some chance of mistakenly classifying individuals as dead. As a consequence, failing to account for falsely-labeled mortality events can significantly bias estimates of mortality rates. To better handle the limitations of underwater telemetry equipment, improve CMR assumptions, deal with animals that have diverse life styles, the use of simulations and models would reduce uncertainties in data interpretations.

Here we focus on the use of telemetry tags to estimate survival rates within a long-term study of three native fish species (Murray cod - *Maccullochella peelii*; trout cod - *Maccullochella macquariensis* and golden perch - *Macquaria ambigua*) in the Murray River, Australia. During this study, individual fish were implanted with radio-telemetry tags. All telemetry tags were equipped with mortality switches, set to go off after a week of inactivity. Yearly telemetry surveys of 300 km of river attempted to find all tagged individuals, and report whether they were alive or dead.

As in other experiments using telemetry tags to infer mortality, we did encounter several problems of state misclassification. First, Murray cod, particularly larger ones, can remain in one location for extended periods, indeed a number of fish that were recorded as dead showed up in later samples as live. Next, due to the varied nature of the habitat and the possibility of fish migrating to side-branches or billabongs, not all fish were found in all years. Finally, while the telemetry tags were set to last for as long as possible, some batteries likely expired. As well, some tags were rendered useless by having their transmitting wire cut at the point of entry (likely by anglers that had captured and released the fish). Consequently, estimates of survival that do not account for false mortality events present in the study are likely to be biased.

Our solution is to treat the scenario as a misclassification problem in a multi-state capture-recapture framework, where individ-

uals can be misclassified as dead when they are actually alive and where detection rates vary between live and dead individuals. Previous work on misclassification problems in CMR studies has shown that by explicitly modelling the probability of misclassifying individuals results in unbiased estimates of transitions between states, including mortality (26; 4), transitions into 'unobservable' states (11; 34) and failed detection of true states (35; 36). Such misclassification work compares with the present study in that the aim of inference is to estimate a biological transition rate of that depends on an observation process that has some degree of error associated with it. However the present study differs from these other contributions in that it is the observation of individuals being alive or dead itself that is possibly mistaken.

Here, we use a Bayesian state-space model to estimate transitions between the states 'alive', 'dead' and 'tag failed' (which includes permanent emigration from the study area), as well as the probability of correctly observing each state. The particulars of the experimental design should apply to a variety of telemetry sampling scenarios. The Murray river dataset are used to show the consequences different assumptions around how individuals move between observable and unobservable states. We also show how variation in sampling conditions can be accommodated in the model. Finally, simulations are used to show how the misclassification model is unbiased under increasingly severe levels of misclassification error.

3. Methods

3.1. Sampling Protocol

Sampling focused on three native predatory fish in the Percichthyidae family: Murray cod, trout cod and golden perch. Murray cod are a large predatory fish in the Percichthyidae family, growing to 2 m in length. Being ambush predators, they often lie under large logs for extended periods waiting for prey (15). Trout cod are closely related to Murray cod, but grow to a smaller size, usually less than 1 m, and tend to occupy slower moving, deeper water river (16; 21). Trout cod are considered endangered, as their main population is restricted to 100 km section of the Murray River, with low numbers found outside this area. Golden perch, also in the Percichthyidae family, are smaller than Murray or trout cod, and tend to occupy lowland reaches of the Murray (8; 17).

Telemetry sampling was undertaken in three main areas of the Murray Darling Basin (figure 1). The upper Murray river (SS3, 120 km) ranges from Lake Hume to the junction of Lake Mulwala. This section of river is degraded, with poor riparian habitat and little in the way of woody habitat that is often used by native fish. Population densities of all three species are lower in this reach than in the others.

[Fig. 1 about here.]

The middle reach (SS1) encompasses Lake Mulwala and the Ovens River below Wangaratta. Lake Mulwala is regarded as Australia's best Murray cod fishery, being a shallow (2 m) lake, while the Ovens river is a slow moving, braided river with abundant riparian and instream habitat. The lower reach (SS2) stretches from Tocumwal, for approximately 100 river km downstream and is regarded as comparatively natural. This reach is home to the largest population of trout cod in Australia.

Fish sampling in each year comprised a two-step process involving initial tagging with a radiotag followed by telemetry surveys. Initial capture of fish involved generator powered pulsator (GPP) Smith-Root boat mounted electrofishing units; details of sampling methods can be found in (18). Between 253 and 424 sites were sampled annually from 2007 and 2012 with each site being defined as a discrete, GPS-marked section of river between 500 and 2000 m in length. Sampling was undertaken between

April and June in each of the study years. While this period was chosen to coincide with low river levels to optimise overall sampling efficiency, year-to-year differences in river flow and depth were likely (19).

Once fish had been captured, they were tagged with both external dart tags and internal passive-internal transponder tags. They were then implanted with radiotags, as per (18). All radio-transmitters (150 MHz frequency) were manufactured by Advanced Telemetry Systems. Three tag types, based on the weight of the fish, were used. For fish that were up to 400 g small transmitters guaranteed to last 4 years were used. For fish between 700 and 900 g, medium-sized transmitters lasting approximately 5 years were used. For the three species involved in this study, a tag burden (or percentage weight of tag relative to fish weight) of 1.5% or less has been shown to produce no noticeable change in behavior or survival (33). Thus, tag were given to fish making sure to keep burden below 1.5% by weight (3). Fish with weight greater than 900 g had the largest transmitters, lasting approximately 6 years. Radio-transmitters were programmed to turn on for one month (May) each year, and turn off for the remaining 11 months. Tagged fish were manually tracked each year during the on-time. The transmitters contained a mortality switch (a mercury motion sensor) which indicated that a fish may have died or shed its transmitter when the fish remained inactive for longer than 7 days. When this switch was thrown, the transmitter emitted a unique signal to indicate a mortality. However, if the fish again started moving, the transmitter resumed with its previous signal. Following capture and implantation of transmitters in each year, a float down survey of the the entire sampling area aimed to detect tagged fish. (18).

3.2. Model Development

Based on the above sampling, we assume that fish are restricted to a defined area and that tracking events occur at regular intervals. We assume that detectability and misclassification rates within the sampling area and between individuals (within a state) is uniform. We ignore tag loss but account for tag failure by allowing individuals to enter a third state 'failed'.

Likelihood: Capture-recapture models of open populations can be conveniently represented in a state-space model, which separates the joint likelihood of the data and parameters into system process and observation models (12; 7; King 2014). In our case, the likelihood can be divided into two components describing 1) the system process for how individuals transition between the alive, dead and tag failed and 2) the observation process, or the likelihood of each of three possible observations given the states of the individuals.

Mathematically, let $y_i = (y_{if_i}, \dots, y_{iT})$ ($i = 1, \dots, N$) be the capture history for each of N tagged individuals between the first time they were observed (f_i) and the last sampling occasion (T). We record $y_{it} = 1$ when an individual was observed as live, $y_{it} = 2$ when it was observed as dead or $y_{it} = 3$ if they went unobserved. Similarly, let $s_i = (s_{if_i}, \dots, s_{iT})$ indicate the true state of individual i at time t , with $s_{it} = 1$ if they were alive, within the sampling site and bearing an active tag at time t , $s_{it} = 2$ if they were dead and bearing an active tag and $s_{it} = 3$ if their tag had failed. Note that we do not distinguish between individuals that are alive and dead after their tag has failed, as these states are indistinguishable without additional data. As well, true tag failure cannot be distinguished here from permanent emigration.

Process model: We model the sequence of states as Markov processes where $\Pr(s_{i,t} = k | s_{i,t-1} = j) = b_{j,k}$. The states are multinomial random variables generated by the process

$$[1] \quad s_{i,t} | s_{i,t-1}, \mathbf{b} \sim \text{Multinomial}(1, b_{s_{i,t-1}})$$

where the notation $b_{s_{it-1}}$ refers to the row in matrix \mathbf{b} corresponding to the state of individual i at time $t - 1$. If the matrix \mathbf{b} is left unconstrained and has more than 2 states, it is not identifiable. Instead, we assume that individuals die with probability μ , cannot transition from dead to alive, and remain in the undetectable state once their tag fails. In CMR literature, the parameter ϕ is often used to denote survival, so here, $\mu = 1 - \phi$. We further assume that the tag failure rate ν is common between alive and dead individuals. Thus, the matrix \mathbf{b} has the form

$$\mathbf{b} = \begin{pmatrix} (1-\mu)(1-\nu) & \mu(1-\nu) & \nu \\ 0 & 1-\nu & \nu \\ 0 & 0 & 1 \end{pmatrix}.$$

Observation model: The observation data y_{it} depend on 1) the probability of detecting individuals given their state and 2) the probability of correctly recording observed states. We let Ψ denote the 3×3 matrix given by

$$\Psi = \begin{pmatrix} p_1\omega & p_1(1-\omega) & 1-p_1 \\ 0 & p_2 & 1-p_2 \\ 0 & 0 & 1 \end{pmatrix}$$

where p_1 and p_2 refer to the probability of detecting live and dead individuals and ω is the probability of correctly recording its state as alive given that it was detected and alive.

The observation process can be written as

$$[2] \quad y_{it}|s_{it}, \Psi \sim \text{Multinomial}(\Psi_{s_{it}})$$

where the subscript notation $\Psi_{s_{it}}$ refers to the row corresponding to state s_{it} . We note that second row in Ψ , denoted Ψ_2 includes no probability of misclassification, reflecting our assumption that dead individuals are never mistaken as alive. Similarly, Ψ_3 reflects that failed transmitters are never observed as alive or dead.

We write the joint posterior distribution of the parameters given the data as

$$[3] \quad [\omega, p, b, s|y] \propto [y|s, w, p][s|\omega, p, b][\omega][p][b]$$

where $[y|..]$ corresponds to the observation process; $[s|...]$ to the state processes and $[\omega]$, $[p]$ and $[b]$ the corresponding (independent) priors.

Application of the full model to native fish in the Murray river: The model as posed above does not account for any variation in mortality rates. However, μ and other parameters can be modified to reflect variation according to different factors. Here, we explore how mortality rates vary between new and old implants, years, stream section and tag sizes. We use the notation $S()Y()$ to denote the state and observation components of the model, including terms μ , ν , ω and p to denote where these parameters are included in the model. Additionally, the model $S(\mu_{TM}.\nu)Y(\omega.p)$ specifies a possibly greater risk of mortality in the first

year post-operation by specifying different values of μ . Similarly, we estimated yearly differences in the μ model by specifying a separate mortality rate for each year of sampling (model $S(\mu_T.\nu)Y(\omega.p)$). A third model estimated μ specific to three different regions of the river (model $S(\mu_R.\nu)Y(\omega.p)$). Finally, transmitters came in three battery sizes, generally corresponding to different sizes of fish and we specified a model that estimates a different transition matrix for three different ranges of tag size (model $S(\mu_L.\nu)Y(\omega.p)$). The rest of the parameters (ν , ω and p) are kept constant over time and over different transmitters. We compared results from each of these four models against a model with constant mortality ($S(\mu.\nu)Y(\omega.p)$) with the deviance information criterion (DIC), and report inter-species differences in parameters estimated for each model.

Comparisons against other classes of models: As the purpose of our model is to account for possible bias due to misclassification, we also compare the model $S(\mu.\nu)Y(\omega.p)$ against three others which made varying assumptions about state transitions and the observation process. First, we explored model $S(\mu.\nu)Y(f.p)$ in which emigration rates were estimated and no misclassification rate is included. We account for obviously mistaken records prior to modelling, using data filtering, a procedure that would have to be used for other CJS models. For example, the observed history of $y_{i,f,1..T} = (1, 3, 2, 1, 2)$ has an obviously mistaken state of dead on occasion $t = 3$, and was changed to $(1, 3, 1, 1, 2)$. The last entry would remain as dead. We next explored model $S(\mu)Y(\omega.p)$ that allows for misclassification but not for tag failure. Thus, we assumed that all failed observations were due to non-detection. This model might apply to a case where the population is assumed to be closed to migration or batteries are expected to last much longer than the duration of the study. Finally, we tested model $S(\mu.\nu)Y(p)$ in which misclassified observations were changed to unobserved data, a situation that might occur if false detections were possible. In this case, the record $(1, 3, 2, 1, 2)$ was changed to $(1, 3, 3, 1, 2)$. Comparisons of model fit were based on the deviance information criterion (DIC) (37)

[Table 1 about here.]

Use of simulations to explore model properties: We use simulations to evaluate bias in μ for models $S(\mu)Y(\omega.p)$ and $S(\mu.\nu)Y(p)$ as well as the full model $S(\mu.\nu)Y(\omega.p)$. We designed simulations based on the process and observation models in equations (1) and (2) and generated data based on two scenarios. First, we set the tag failure rate ν to vary between 0 and 0.4 while the misclassification rate ω stayed constant at 0.25. Next, we produced data where ω varied between 0 and 0.4 but ν remained at 0.3. For each level of ν and ω , we simulated 500 datasets of 500 individuals across 8 years of sampling, then estimated μ for each of the four model classes described above.

Parameter Estimation using MCMC We used the BUGS programming language to sample from the joint posterior distribution of the parameters given the data. All models and simulations were written in the programming language R (27). All MCMC sampling was done using the program JAGS (22) accessed through the R package 'R2jags' (31). Simulations were run on a multi-core processor using the package 'doSNOW' (1). For all models, we ran three chains of 50,000 iterations each, for a total of 30,000 samples. Convergence of chains was assessed using the Gelman-Rubin diagnostic in the package 'coda' (23).

4. Results

4.1. Murray river data:

We deployed between 22 (trout cod, 2009) and 159 (Murray cod, 2008) transmitters per species each year, for a total of 1317 transmitters deployed (table 2) across fish in the three size classes (table 3).

[Table 2 about here.]

[Table 3 about here.]

Transmitters in trout cod were observed to have been erroneously misclassified as dead the least frequently (maximum = 0.02), while misclassification rates of transmitters in Murray cod and Golden perch were misclassified more often (0.25 and 0.3; table 5). These would represent a lower bound for the estimated true misclassification rate.

[Table 4 about here.]

When comparing between model types, several clear trends were apparent across all species, though these trends were only strong (as evidenced by a lack of overlap in 95% credible intervals) in certain species. In general, none of the trends observed were significant for trout cod, so we limit our discussion of the results to golden perch and Murray cod. First, as expected, including the misclassification term ω (models $S(\mu)Y(\omega.p)$ and $S(\mu.\nu)Y(\omega.p)$) resulted in lower values of μ . The differences were marked in golden perch, with no overlap in the 95% credible intervals between these two classes of models only marginal overlap for Murray cod (figure 2 A-C). Within the models that included a misclassification term ω , including the tag failure parameter ν resulted in much lower estimates of ω for golden perch, and only slightly lower ω in Murray (figure 2 D-F). Including a tag failure term ω also resulted in higher ν in both golden perch and Murray cod (figure 2 G-I). Finally, detection rates tended to be vastly underestimated for live fish when ν was not included (model $S(\mu)Y(\omega)$, figure 2 J-L). As well, detection rates tended to be higher for live fish than for dead fish in both golden perch and Murray cod.

Comparing μ between stream sections showed that for Murray cod, μ was higher in SS1, whereas there was little discernible difference for other species (figure 3A). We found that μ was much higher (0.15 vs 0.05) in newly tagged golden perch and slightly higher in Murray cod ($\mu = 0.075$ vs 0.038) (figure 3B). Fish with smaller transmitters tended to have higher μ (figure 3C), but this was not a strong trend. Finally, between all years, 2008 had the highest mortality rates for golden perch, whereas there was no clear distinction for Murray cod (figure 3D).

Each of the three species had a different model for μ that provided the best fit to the data. For Murray cod, the model that included no partitioning of mortality between different groups ($S(\mu.\nu)Y(\omega.p)$) had the lowest DIC (=2871). In trout cod, the including tag size as a factor $S(\mu_{TS}.\nu)Y(\omega.p)$ resulted in the lowest DIC (=550) and in golden perch, the lowest DIC was found for the tag mortality model $S(\mu_{TM}.\nu)Y(\omega.p)$ (DIC=1547) (table 5).

4.2. Simulated data

Our simulations indicate that failing to account for either tag detection or misclassification biases mortality estimates. As the tag failure rate ν increases (while maintaining state-dependent capture probabilities p , tag failure ν and misclassification rates ω constant), the estimates of mortality rates (μ) from model $S(\mu)Y(\omega.p)$ become increasingly biased (figure 4 A) and the probability of detecting dead individuals (p_2) is increasingly negatively biased (figure 4 B). By contrast, in model $S(\mu.\nu)Y(\omega.p)$ estimates of mortality and detection rates are consistently centred around the true values (figure 4 C, D). For model $S(\mu.\nu)Y(p)$, μ is biased downwards, as are estimates of p_1 and p_2 (figure 4 E, F).

When we varied ω while maintaining constant p , ν and μ , $S(\mu)Y(\omega)$ returned biased μ , but this decreased as ω increased (figure 5 A). Tag detection rates p in this model remained consistently biased, though estimated detection of dead individuals

(p_2) was more heavily biased than for alive individuals p_1 (figure 5 B). Model $S(\mu.\nu)Y(\omega.p)$ continued to provide estimates of detection and survival that were centred around the true values (figure 5 C, D). In model $S(\mu.\nu)Y(p)$, mortality rates were biased downwards, as were detection rates (figure 5 E, F)

In simulations that varied p while maintaining constant μ , ν and ω , model $S(\mu)Y(\omega.p)$ consistently overestimated mortality and underestimated detection for dead individuals (figure 6 A, B). Mortality estimates from model $S(\mu.\nu)Y(\omega.p)$ again were consistent with the true values (figure 6 C, D), while model $S(\mu.\nu)Y(p)$ underestimated both μ and p (figure 6 E, F).

[Fig. 2 about here.]

[Fig. 3 about here.]

[Table 5 about here.]

[Fig. 4 about here.]

[Fig. 5 about here.]

[Fig. 6 about here.]

5. Discussion

Identifying mortality events using telemetry or other remote observations is a powerful tool in ecology, particularly where standard capture techniques are labour intensive or have a low success rate. However, confusing normal behavioural patterns with death can bias estimates of mortality. Here, we account for such misclassification using a model similar to the multi-event or misclassification models (26; 11; 10; 14). Setting this problem in a state-space framework allows for clearer distinction between the observation and process models, making it possible to extend the model to a variety of different scenarios.

Using this approach, we were able to estimate the impact of tag implantation on mortality rates in wild fish, with newly-tagged individuals more likely to die than those that have had the tag implanted for more than a year. This finding supports other work showing that the stress of implantation should be considered in future radiotagging study design (29; 24). In addition, we show how mortality rates vary between different parts of a river, differently-sized fish and between years. Our results indicate that for Murray cod, individuals with small transmitters have the highest mortality rates, likely a consequence of the relatively greater vulnerability of small fish to the shock of implantation. By contrast, golden perch implanted with medium-size transmitters that had the highest mortality rates in that species. Year-to-year variation in μ appears small for both Murray cod and golden perch, with the exception of 2008 for golden perch, which may be explained by the greater proportion of newly tagged individuals at the start of the study. As well, mortality in 2012 appears lower in both species. Results for Trout cod had very wide credible intervals indicating that sample sizes were too small to interpret meaningful results from these data.

In this study, we allowed for variability in mortality rates between different groups of fish. Modifications are possible to allow for variability in misclassification and detection rates as well. Indeed, we note that allowing for differential detection of alive and dead fish appears to be an important consideration. In our simulations, we found that failing to account for misclassification (but still modelling tag failure) significantly underestimates μ . In these scenarios, we set the detection rate for live individuals at

$p_1 = 0.3$ and $p_2 = 0.2$ and as a consequence individuals with failed transmitters are more likely to look as though they are dead. This bias would overestimate population size and the rate of population turnover in full population models. By contrast, models that account for tag mortality but not tag misclassification tend to underestimate mortality rates and detection rates, inflating the size and longevity of populations. We also showed that failing to include tag failure rates (model $S(\mu)Y(\omega.p)$) has the strongest influence on μ and p , resulting in a strong bias with even relatively low ν . Conversely, the model that did include tag failure and tag misclassification (model $S(\mu,\nu)Y(p)$) was relatively robust to increasing misclassification bias.

Further generalisations are in principle possible to allow for misclassification in a variety of other scenarios. For example, false survival and false mortality can be accommodated by adjusting the misclassification vector ω (30). However, either additional assumptions concerning the probabilities of misclassification rates or additional observations of individuals in each state are required. For example, one could provide the model with reference data or prior information against which to calibrate the misclassification rates with new data. While this model is framed in terms of detecting telemetry transmitters, the model is useful in a wider range of contexts. Misclassification models have been used to explore a things such as disease state transitions (4) in imperfectly detected individuals, as well as the reproductive status of wild animals (10; 2) and migration rates (26). Our state-space model is applicable to both these scenarios.

On a final note, we note that the usual caveats concerning the modelling approach being valid only when the relevant underlying assumptions are true. For instance, we assume that all transmitters are detected equally within the study region. Modifications to this and other assumptions could be allowed, but would have to be accounted for in the experimental design and the model modified accordingly.

References

1. Analytics, R. (2012) *doSNOW: Foreach parallel adaptor for the snow package*. R package version 1.0.6.
2. Avril, A., Letty, J., Pradel, R., Leonard, Y., Santin-Janin, H. & Pontier, D. (2012) A multi-event model to study stage-dependent dispersal in radio-collared hares: when hunting promotes costly transience. *Ecology* **93**, 1305–1316.
3. Bacheler, N.M., Buckel, J.A., Hightower, J.E., Paramore, L.M. & Pollock, K.H. (2009) A combined telemetry - tag return approach to estimate fishing and natural mortality rates of an estuarine fish. *Canadian Journal of Fisheries and Aquatic Sciences* **66**, 1230–1244.
4. Conn, P.B. & Cooch, E.G. (2009) Multistate capture-recapture analysis under imperfect state observation: an application to disease models. *Journal of Applied Ecology* **46**, 486–492.
5. Donaldson, M.R., Arlinghaus, R., Hanson, K.C. & Cooke, S.J. (2008) Enhancing catch-and-release science with biotelemetry. *Fish and Fisheries* **9**, 79–105.
6. Friedl, S., Buckel, J., Hightower, J., Scharf, F. & Pollock, K. (2013) Telemetry-based mortality estimates of juvenile spot in two north carolina estuarine creeks. *Transactions of the American Fisheries Society* **142**, 399 – 415.
7. Gimenez, O., Rossi, V., Choquet, R., Dehais, C., Doris, B., Varella, H., Vila, J.P. & Pradel, R. (2007) State-space modelling of data on marked individuals. *Ecological Modelling* **206**, 431–438.

- 281 8. Humphries, P., King, A. & Koehn, J. (1999) Fish, flows and flood plains: links between freshwater fishes and their environ-
282 ment in the Murray-Darling River system, Australia. *Environmental Biology of Fishes* **56**, 129–151.
- 283 9. Kawabata, Y., Asami, K., Kobayashi, M., Sato, T., Okuzawa, K., Yamada, H., Yoseda, K. & Arai, N. (2011) Effect of
284 shelter acclimation on the post-release movement and putative predation mortality of hatchery-reared black-spot tuskfish
285 *choerodon schoenleinii*, determined by acoustic telemetry. *Fisheries Science* **77**, 345 – 355.
- 286 10. Kendall, W.L., White, G.C., Hines, J.E., Langtimm, C.A. & Yoshizaki, J. (2012) Estimating parameters of hidden markov
287 models based on marked individuals: use of robust design data. *Ecology* **93**, 913 – 920.
- 288 11. Kendall, W., Hines, J. & Nichols, J. (2003) Adjusting multistate capture-recapture models for misclassification bias: Man-
289 atee breeding proportions. *Ecology* **84**, 1058–1066.
- 290 12. King, R. (2012) A review of Bayesian state-space modelling of capture-recapture-recovery data. *Interface Focus* **2**, 190–204.
- 291 King, R. (2014) Statistical Ecology. *Annual Review of Statistics and its Application* **1**, 40–426.
- 292 14. King, R. & McCrea, R.S. (2014) A generalised likelihood framework for partially observed capture–recapture–recovery
293 models. *Statistical Methodology* **17**, 30–45.
- 294 15. Koehn, J.D., McKenzie, J.A., O’Mahony, D.J., Nicol, S.J., O’Connor, J.P. & O’Connor, W.G. (2009) Movements of Murray
295 cod (*Maccullochella-peelii*) in a large Australian lowland river. *Ecology of Freshwater Fish* **18**, 594–602.
- 296 16. Koehn, J.D. (2009) Using radio telemetry to evaluate the depths inhabited by Murray cod (*Maccullochella peelii peelii*).
297 *Marine and Freshwater Research* **60**, 317–320.
- 298 17. Lintermans, M. (2007) *Fishes of the Murray-Darling Basin: an introductory guide*. Murray-Darling Basin Commission
299 Canberra.
- 300 18. Lyon, J.P., Bird, T., Nicol, S., Kearns, J., O’Mahony, J., Todd, C.R., Cowx, I.G., Bradshaw, C.J. & Jech, J.M. (2014) Effi-
301 ciency of electrofishing in turbid lowland rivers: implications for measuring temporal change in fish populations. *Canadian*
302 *Journal of Fisheries and Aquatic Sciences* **71**, 878–886.
- 303 19. Lyon, J.P., Todd, C., Nicol, S.J., MacDonald, A., Stoessel, D., Ingram, B.A., Barker, R.J. & Bradshaw, C.J. (2012) Rein-
304 troduction success of threatened australian trout cod (*maccullochella macquariensis*) based on growth and reproduction.
305 *Marine and Freshwater Research* **63**, 598–605.
- 306 20. Nasution, M., Brownie, C., Pollock, K. & Bennetts, R. (2001) Estimating survival from joint analysis of resighting and
307 radiotelemetry capture-recapture data for wild animals. *Journal of Agricultural Biological and Environmental Statistics* **6**,
308 461–478.
- 309 21. Nicol, S.J., Batker, R.J., Koehn, J.D. & Burgman, M.A. (2007) Structural habitat selection by the critically endangered trout
310 cod, *Maccullochella macquariensis*, Cuvier. *Biological Conservation* **138**, 30–37.
- 311 22. Plummer, M. (2003) *JAGS: A program for analysis of Bayesian graphical models using Gibbs sampling*.

23. Plummer, M., Best, N., Cowles, K. & Vines, K. (2006) Coda: Convergence diagnosis and output analysis for mcmc. *R News* **6**, 7–11.
24. Pollock, K.H. & Pine, III, W.E. (2007) The design and analysis of field studies to estimate catch-and-release mortality. *Fisheries Management and Ecology* **14**, 123–130, 135th Annual Meeting of the American-Fisheries-Society Symposium, Anchorage, AK, SEP 11-15, 2006.
25. Pollock, K.H. (1991) Modeling capture, recapture, and removal statistics for estimation of demographic parameters for fish and wildlife populations: Past, present, and future. *Journal of the American Statistical Association* **86**, 225–238.
26. Pradel, R. (2005) Multievent: An extension of multistate capture-recapture models to uncertain states. *Biometrics* **61**, 442–447.
27. R Development Core Team (2013) *R: A Language and Environment for Statistical Computing*. R Foundation for Statistical Computing, Vienna, Austria, ISBN 3-900051-07-0.
28. Kordjazi, Ziya & Frusher, Stewart & Buxton, Colin & Gardner, Caleb & Bird, Tomas (2016) The Influence of Mark-Recapture Sampling Effort on Estimates of Rock Lobster Survival. *PloS one* **11**, 3.
29. Rechisky, E.L. & Welch, D.W. (2010) Surgical implantation of acoustic tags: Influence of tag loss and tag-induced mortality on free-ranging and hatchery-held spring chinook (*Oncorhynchus tshawytscha*) smolts. *PNAMP special publication: tagging, telemetry and marking measures for monitoring fish populations—a compendium of new and recent science for use in informing technique and decision modalities* **2**, 69–94.
30. Royle, J.A. & Link, W.A. (2006) Generalized site occupancy models allowing for false positive and false negative errors. *Ecology* **87**, 835–841.
31. Su, Y.S. & Yajima, M. (2011) *R2jags: A Package for Running jags from R*. R package version 0.02-15.
32. Thorstad, E.B., Uglem, I., Arechavala-Lopez, P., ØKland, F. & Finstad, B. (2011) Low survival of hatchery-released atlantic salmon smolts during initial river and fjord migration. *Boreal Environment Research* **16**, 115 – 120.
33. O'Connor, JP & Koehn, JD & Nicol, SJ & O'Mahony, DJ & McKenzie, JA(2010) Retention of radio tags in golden perch (*Macquaria ambigua*), silver perch (*Bidyanus bidyanus*) and carp (*Cyprinus carpio*). *Marine and Freshwater Research* **60**,3, 334–340.
34. Barbraud, C and Weimerskirch, H, (2010) Estimating survival and reproduction in a quasi-biennially breeding seabird with uncertain and unobservable states. *Journal of Ornithology* **152**,2, 605–615.
35. Miller, David AW and Talley, Brooke L and Lips, Karen R and Campbell Grant, Evan H, (2012) Estimating patterns and drivers of infection prevalence and intensity when detection is imperfect and sampling error occurs. *Methods in Ecology and Evolution* **3**,5, 850–859.

- 342 36. Choquet, Rémi and Carrié, Cécile and Chambert, Thierry and Boulinier, Thierry, (2013) Estimating transitions between
343 states using measurements with imperfect detection: application to serological data. *Ecology* **94**,10, 2160–2165.
- 344 37. Spiegelhalter, DJ and Best, NG and Carlin, BP and Van Der Linde, A, (2002) Bayesian measures of model complexity and
345 fit. *Journal of the Royal Statistical Society: Series B (Statistical Methodology)* **64**,4, 583–639.

List of Figures

346	1	Study location mapped in relation to the Murray-Darling basin (light grey) and the rest of Australia.	14
347	2	Posterior mean (symbols) and 95% credible intervals (vertical segments) for survival (μ), misclassification (ω),	
348		tag failure (ν) and detection (p , red=dead, green=alive) parameters in each of the four models described in the text	
349		for the three species used in this study. GP= golden perch, MC=Murray cod, TC=trout cod.	15
350	3	Posterior mean (symbols) and 95% credible intervals (vertical segments) for different models in each of the three	
351		species. GP= golden perch, MC=Murray cod, TC=trout cod. Models tested included μ varying with stream section	
352		(A), fish with new (≤ 1 Year) and old transmitters (B), three different sizes of transmitters (C) and over the 5 years	
353		for which μ was estimable (D)	16
354	4	Boxplots of posterior mean values for mortality rates (panels A,C and E) and detection parameters (panels B,D	
355		and F) at varying levels of tag failure for misclassification-only ($S(\mu,\nu)Y(\omega)$, panels A and B), misclassification	
356		+ tag failure ($S(\mu,\nu)Y(\omega,p)$, panels C and D) and tag failure only ($S(\mu,\nu)Y(p)$, panels E and F). Boxes indicate	
357		the 25 and 75% posterior quantiles of survival estimates from 200 simulated datasets at each level of tag failure.	
358		In panels E and F, estimated detection rates are shown for both alive (p_1 , red) and dead (p_2 , green) individuals.	
359		Solid horizontal lines on panels A,C and E indicate the true mortality rates (μ) used in the simulations, while on	
360		panels B, D and F, horizontal dashed and solid lines indicate true detection rates p_1 and p_2	17
361	5	Boxplots of posterior mean values for mortality rates (panels A,C and E) and detection parameters (panels B,	
362		D and F) at varying levels of tag misclassification for misclassification-only ($S(\mu)Y(\omega,p)$, panels A and B),	
363		misclassification + tag failure ($S(\mu,\nu)Y(\omega,p)$, panels C and D) and tag failure only ($S(\mu,\nu)Y(p)$, panels E and	
364		F). Boxes indicate the 25 and 75% posterior quantiles of μ from 500 simulated datasets at each level of tag failure.	
365		In panels E and F, estimated detection rates are shown for both alive (p_1 , red) and dead (p_2 , green) individuals.	
366		Solid horizontal lines on panels A,C and E indicate the true mortality rates (μ) used in the simulations, while on	
367		panels B, D and F, horizontal dashed and solid lines indicate true detection rates p_1 and p_2	18
368	6	Boxplots of posterior mean values for mortality rates (panels A, C and E) and detection parameters (panels B, D	
369		and F) at varying levels of tag detection for misclassification-only ($S(\mu)Y(\omega,p)$, panels A and B), misclassification	
370		+ tag failure ($S(\mu,\nu)Y(\omega,p)$, panels C and D) and tag failure only ($S(\mu,\nu)Y(p)$, panels E and F). Boxes indicate	
371		the 25 75% posterior quantiles of survival estimates from 500 simulated datasets at each level of tag failure. In	
372		panels E and F, bias in estimated detection rates are shown for both alive (p_1 , red) and dead (p_2 , green) individuals.	19
373			

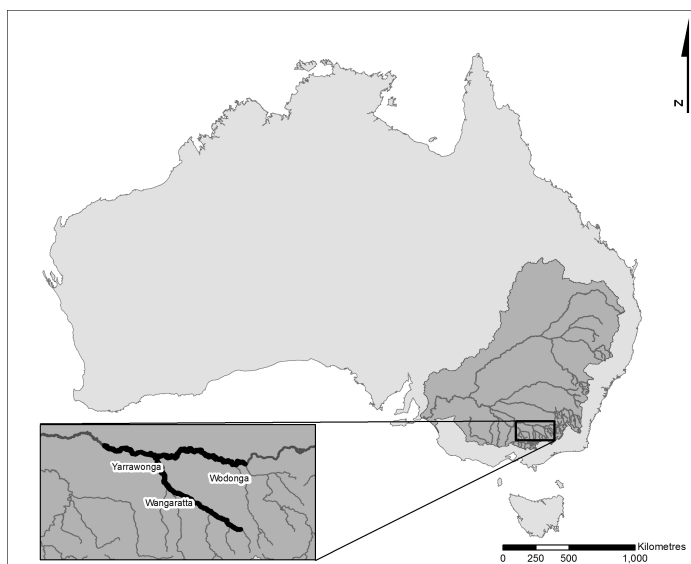


Fig. 1. Study location mapped in relation to the Murray-Darling basin (light grey) and the rest of Australia.

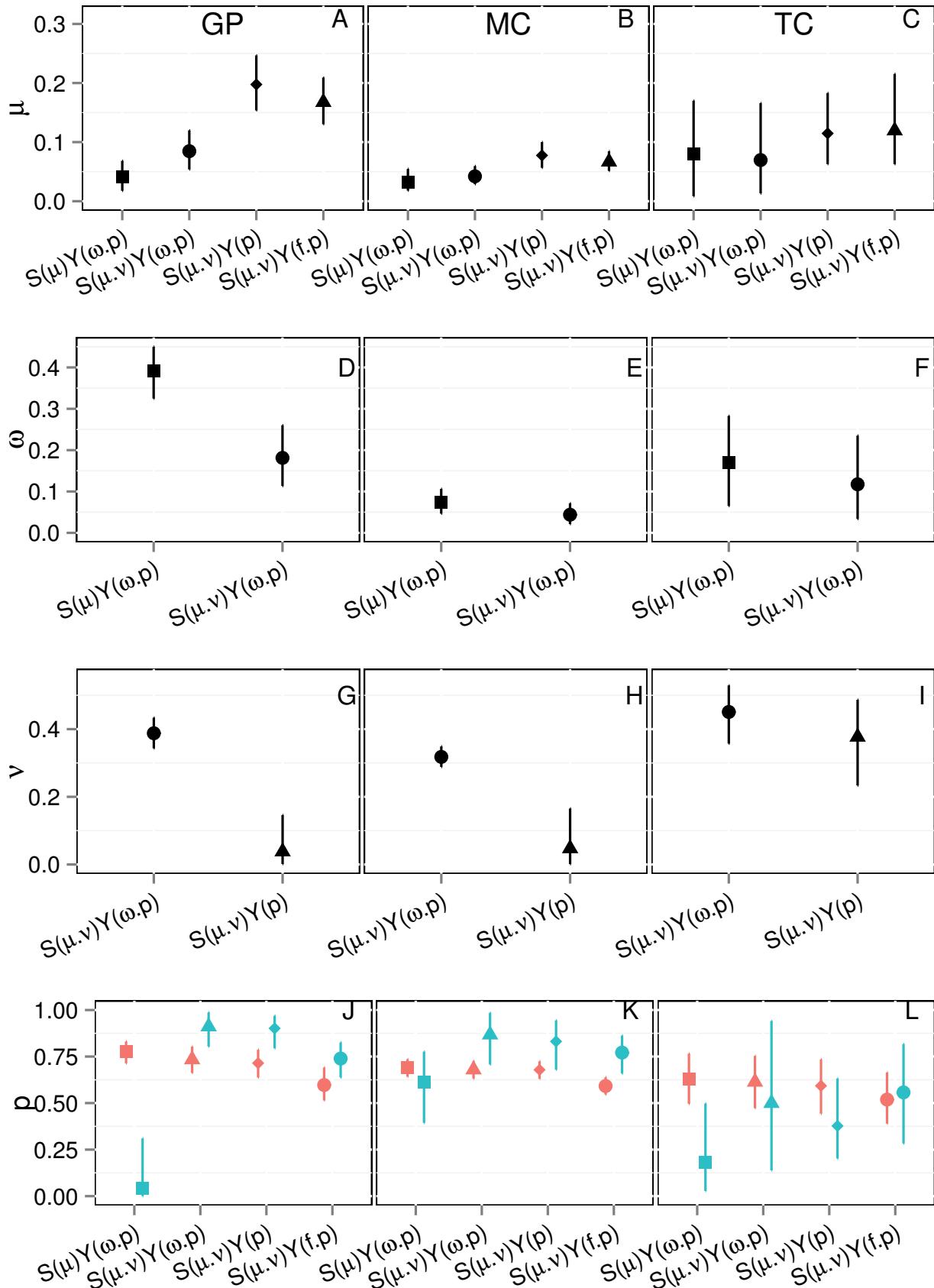


Fig. 2. Posterior mean (symbols) and 95% credible intervals (vertical segments) for survival (μ), misclassification (ω), tag failure (ν) and detection (p , red=dead, green=alive) parameters in each of the four models described in the text for the three species used in this study. GP= golden perch, MC=Murray cod, TC=trout cod.

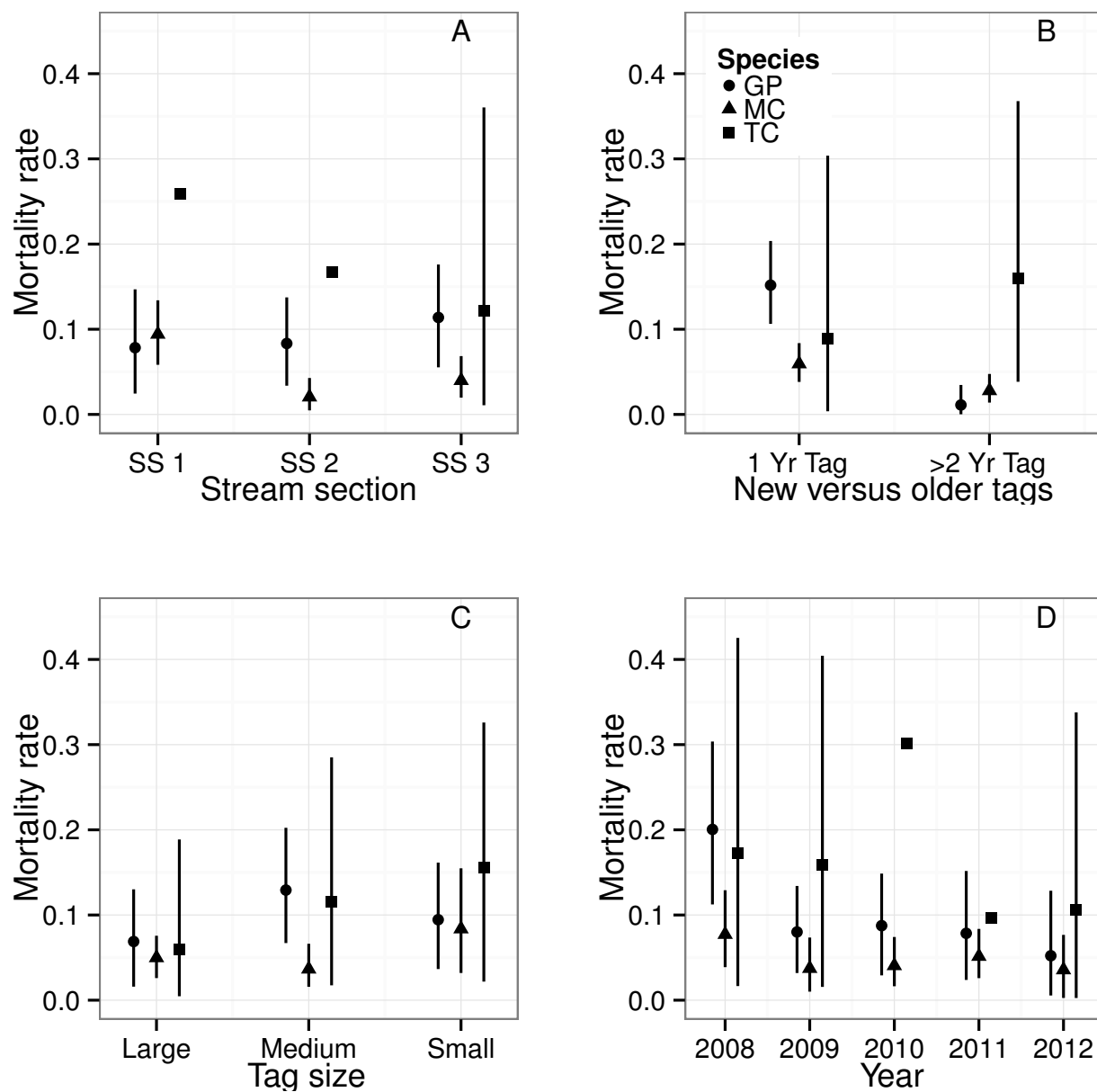


Fig. 3. Posterior mean (symbols) and 95% credible intervals (vertical segments) for different models in each of the three species. GP= golden perch, MC=Murray cod, TC=trout cod. Models tested included μ varying with stream section (A), fish with new (<1 Year) and old transmitters (B), three different sizes of transmitters (C) and over the 5 years for which μ was estimable (D)

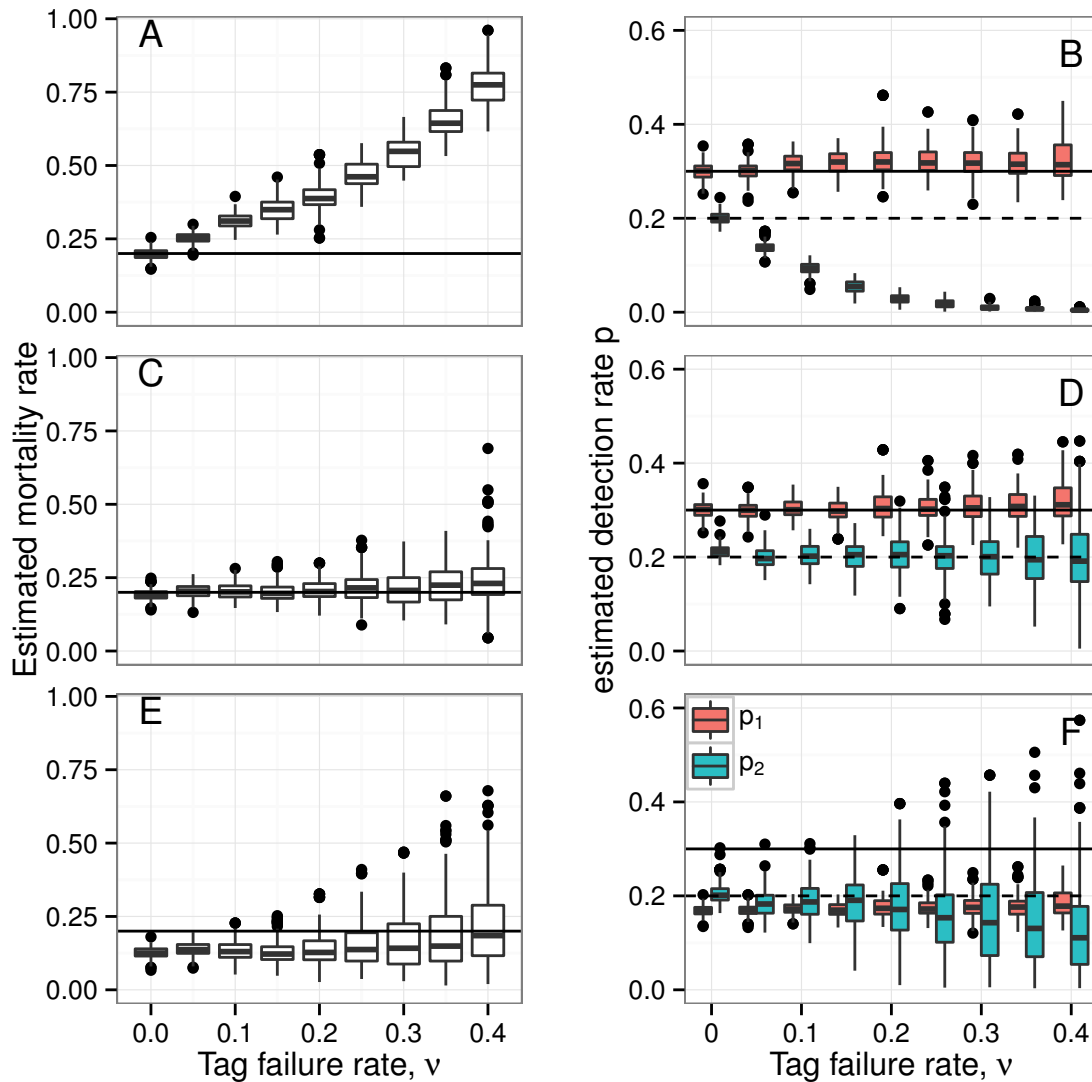


Fig. 4. Boxplots of posterior mean values for mortality rates (panels A,C and E) and detection parameters (panels B,D and F) at varying levels of tag failure for misclassification-only ($S(\mu,\nu)Y(\omega)$, panels A and B), misclassification + tag failure ($S(\mu,\nu)Y(\omega,p)$, panels C and D) and tag failure only ($S(\mu,\nu)Y(p)$, panels E and F). Boxes indicate the 25 and 75% posterior quantiles of survival estimates from 200 simulated datasets at each level of tag failure. In panels E and F, estimated detection rates are shown for both alive (p_1 , red) and dead (p_2 , green) individuals. Solid horizontal lines on panels A,C and E indicate the true mortality rates (μ) used in the simulations, while on panels B, D and F, horizontal dashed and solid lines indicate true detection rates p_1 and p_2 .

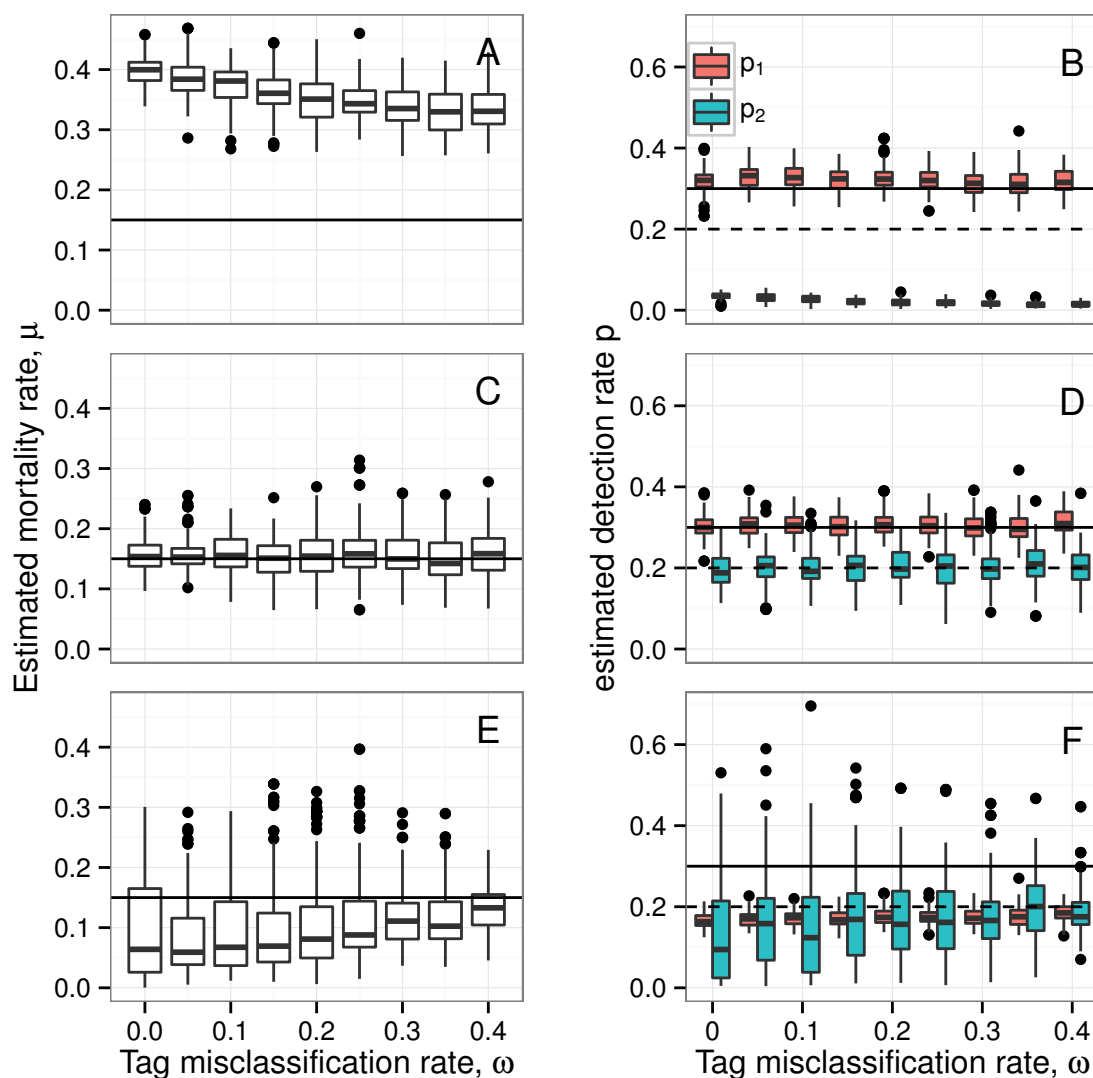


Fig. 5. Boxplots of posterior mean values for mortality rates (panels A,C and E) and detection parameters (panels B, D and F) at varying levels of tag misclassification for misclassification-only ($S(\mu)Y(\omega.p)$, panels A and B), misclassification + tag failure ($S(\mu.\nu)Y(\omega.p)$, panels C and D) and tag failure only ($S(\mu.\nu)Y(p)$, panels E and F). Boxes indicate the 25 and 75% posterior quantiles of μ from 500 simulated datasets at each level of tag failure. In panels E and F, estimated detection rates are shown for both alive (p_1 , red) and dead (p_2 , green) individuals. Solid horizontal lines on panels A,C and E indicate the true mortality rates (μ) used in the simulations, while on panels B, D and F, horizontal dashed and solid lines indicate true detection rates p_1 and p_2 .

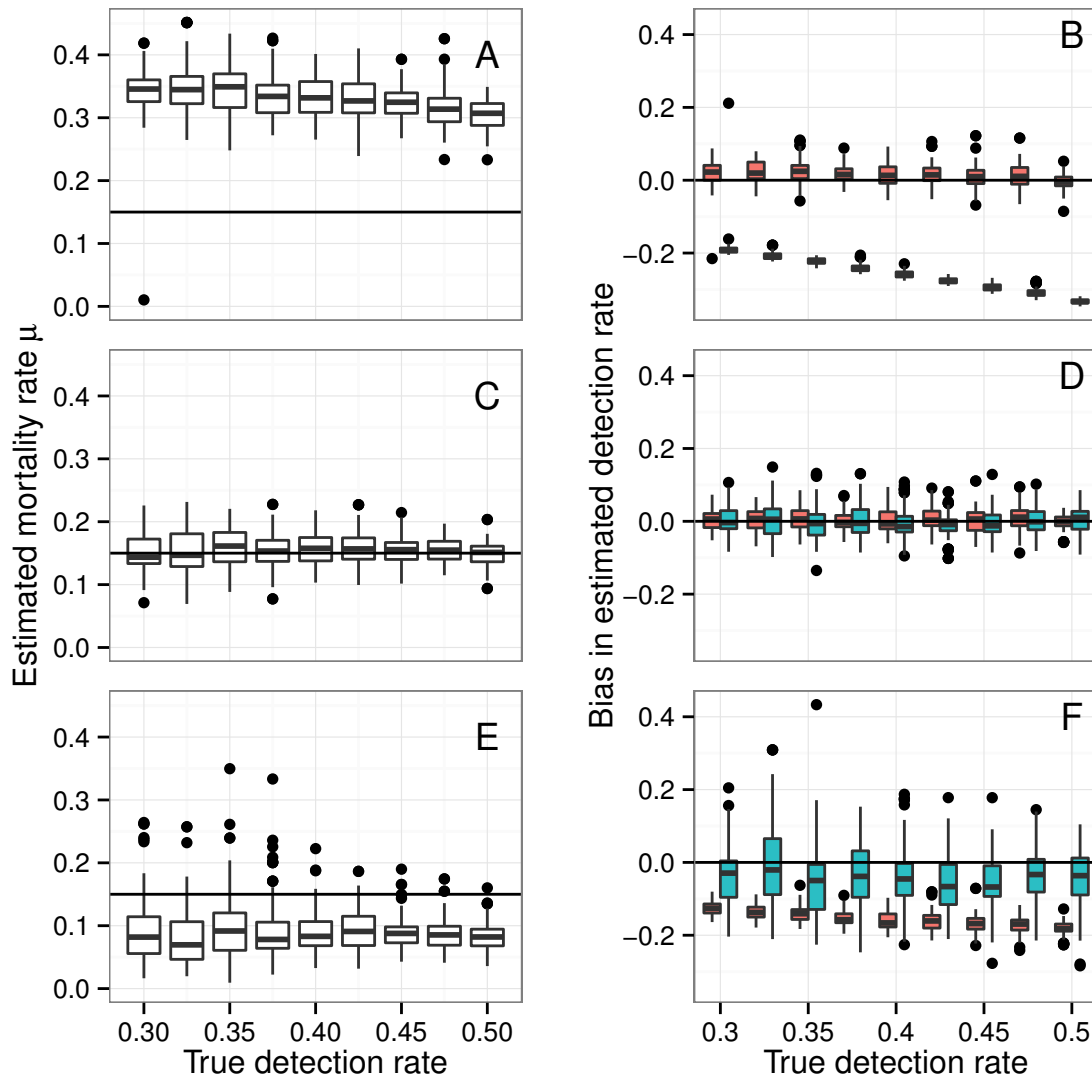


Fig. 6. Boxplots of posterior mean values for mortality rates (panels A, C and E) and detection parameters (panels B, D and F) at varying levels of tag detection for misclassification-only ($S(\mu)Y(\omega.p)$, panels A and B), misclassification + tag failure ($S(\mu.\nu)Y(\omega.p)$, panels C and D) and tag failure only ($S(\mu.\nu)Y(p)$, panels E and F). Boxes indicate the 25 75% posterior quantiles of survival estimates from 500 simulated datasets at each level of tag failure. In panels E and F, bias in estimated detection rates are shown for both alive (p_1 , red) and dead (p_2 , green) individuals.

List of Tables

374	1	Summary of models explored. Subscripts on the parameters μ , ν , ω , and p indicate models testing different hypotheses.	21
375			
376	2	Numbers of transmitters deployed in each streamsection for each species across the 6 years of the study	22
377			
378	3	Mean fish lengths, battery sizes and tag burden for implanted transmitters in each of the three species included in this study. Length and size ranges are given in square brackets.	23
379			
380	4	Summary of telemetry tag data recorded in the Murray river dataset. Tag observations are recorded for three species: Murray cod, trout cod and golden perch in years 2007-2012. extbfT.A.L= number of tags assumed to be operational on manufacturers guaranteed battery expiry dates. extbfAlive = fish observed alive, extbfDead = fish observed dead, extbfMisclassified = number of tags that were classified as dead but later appeared as alive. Numbers of tags in S/M/L size classes are shown. For 2012, no known misclassifications could occur.	24
381			
382			
383			
384			
385	5	Deviance information criterion (DIC) values for five different parameterizations of the $S(\mu.\nu)Y(\omega.p)$ model for each Murray cod (<i>MC</i>), trout cod (<i>TC</i>) and golden perch (<i>GP</i>).	25
386			

Table 1. Summary of models explored. Subscripts on the parameters μ , ν , ω , and p indicate models testing different hypotheses.

Model notation	Name	Hypothesis
$S(\mu.\nu)Y(\omega.p)$	Base model	Parameters equal across all fish
$S(\mu_{TM}.\nu)Y(\omega.p)$	Tag mortality	Mortality is different in first year post-tagging compared to subsequent years
$S(\mu_Y.\nu)Y(\omega.p)$	Yearly	Mortality varies between years
$S(\mu_R.\nu)Y(\omega.p)$	River Section	Mortality varies between river sections
$S(\mu_{TS}.\nu)Y(\omega.p)$	Fish Size	Mortality varies with fish size
$S(\mu.\nu)Y(f.p)$	Misclassification corrected	Misclassification errors filtered manually
$S(\mu.\nu)Y(f.p)$	No tag failure	Tag failure ignored (all failed detections treated equally)
$S(\mu.\nu)Y(p)$	Misclassifications ignored	Misclassifications treated as missing data

Table 2. Numbers of transmitters deployed in each streamsection for each species across the 6 years of the study

	SS1	SS2	SS3	Total
Murray Cod	199	274	205	678
Trout Cod	3	192	17	212
Golden Perch	109	190	119	418
Total	311	656	341	1308

Species	Battery Size	N	Total Length (mm)	Battery Weight (g)	Tag Burden (%)
Golden Perch	Large	70	490 [412,581]	1182 [1120,1460]	0.03 [0.005, 0.7]
Golden Perch	Medium	81	463 [335,575]	902 [700,950]	0.1 [0.02, 1.4]
Golden Perch	Small	194	409 [278,621]	414 [230,600]	0.7 [0.5, 1.5]
Murray Cod	Large	29	835 [501,1228]	2250 [2250,2250]	0.08 [0.01, 0.2]
Murray Cod	Medium	255	658 [383,1280]	1203 [950,1460]	0.25 [0.15, 0.7]
Murray Cod	Small	325	431 [288,1058]	432 [230,900]	0.4 [0.4, 1.4]
Trout Cod	Large	26	516 [414,605]	1035 [900,1250]	0.1 [0.01, 0.55]
Trout Cod	Medium	25	457 [388,550]	613 [517,871]	0.2 [0.05, 0.75]
Trout Cod	Small	117	366 [239,487]	251 [150,400]	0.5 [0.01, 1.5]

Table 3. Mean fish lengths, battery sizes and tag burden for implanted transmitters in each of the three species included in this study. Length and size ranges are given in square brackets.

years	NewTags	TotalTags	ObsAlive	ObsDead	MistDead
2007	161	90/36/35	0/0/0	0/0/0	0.00
2008	131	127/81/81	5/10/5	4/6/5	3.00
2009	105	73/89/140	26/27/36	3/9/2	5.00
2010	106	33/75/206	7/18/69	1/9/8	3.00
2011	77	15/69/227	3/30/98	0/10/9	0.00
2012	65	15/64/213	2/22/91	0/7/12	0.00
2007	45	31/13/1	0/0/0	0/0/0	0.00
2008	34	49/18/12	4/4/1	4/1/0	1.00
2009	22	41/16/14	9/7/6	2/3/0	0.00
2010	34	41/14/15	3/5/5	2/2/4	1.00
2011	32	45/11/20	2/5/6	0/0/2	0.00
2012	28	58/18/13	4/6/5	0/0/2	0.00
2007	87	46/31/10	0/0/0	0/0/0	0.00
2008	94	67/68/44	5/4/3	7/14/0	1.00
2009	49	29/75/68	5/19/21	4/10/8	4.00
2010	58	16/56/94	4/14/25	3/11/16	6.00
2011	57	16/52/114	3/15/31	0/14/14	3.00
2012	73	25/64/89	2/15/24	0/12/13	0.00

Table 4. Summary of telemetry tag data recorded in the Murray river dataset. Tag observations are recorded for three species: Murray cod, trout cod and golden perch in years 2007-2012. extbfT.A.L= number of tags assumed to be operational on manufacturers guaranteed battery expiry dates. extbfAlive = fish observed alive, extbfDead = fish observed dead, extbfMisclassified = number of tags that were classified as dead but later appeared as alive. Numbers of tags in S/M/L size classes are shown. For 2012, no known misclassifications could occur.

Table 5. Deviance information criterion (DIC) values for five different parameterizations of the $S(\mu.\nu)Y(\omega.p)$ model for each Murray cod (*MC*), trout cod (*TC*) and golden perch (*GP*).

Model	Notation	GP	MC	TC
Base	$S(\mu.\nu)Y(\omega.p)$	1701	2871	784
Tag Mortality	$S(\mu_{TM}.\nu)Y(\omega.p)$	1547	3138	895
Year	$S(\mu_Y.\nu)Y(\omega.p)$	1784	2887	723
Tag Size	$S(\mu_{TS}.\nu)Y(\omega.p)$	1834	2892	550
Stream Section	$S(\mu_{SS}.\nu)Y(\omega.p)$	1726	2983	746